

# IMAGE PROCESSING OPTIMIZATION OF 2D RESISTIVITY DATA FOR MODELING ANOMALOUS ZONES OF PHOSPHATE «DISTURBANCES»

## OPTIMIZACIÓN DE PROCESAMIENTO DE IMÁGENES DE DATA DE RESISTIVIDAD 2D PARA MODELADO DE ZONAS ANÓMALAS DE FOSFATOS “DISTURBADOS”

Saad Bakkali\*, Mahacine Amrani\*\*

### ABSTRACT

A Schlumberger resistivity survey over an area of 50 hectares was carried out. A new field procedure based on analytic signal response of resistivity data was tested to deal with the presence of phosphate deposit disturbances. Models of the geology were successfully obtained from surface modeling of 2D peaks of resistivity data. Image processing optimization was based on surface optimization tools. Downward analytical prolongation of the surface modeling along 30 meters of depth was used for modeling optimization. Analytical procedures were found to be consistently useful. Optimization of phosphate reserves were improved and better constrained.

**Keywords:** resistivity, phosphate, surface modeling, analytic signal, downward, Morocco.

### RESUMEN

Un registro de resistividad Schlumberger fue realizado sobre un área de 50 hectáreas. Un nuevo campo de procesos basados en la respuesta de la señal analítica de la data de resistividad fue probada en presencia de depósitos de fosfatos disturbados. Modelos de geología fueron sucesivamente obtenidos desde un modelo de los picos de la data de resistividad 2D. La optimización del proceso de imágenes fue basada en la optimización de herramientas de superficie. La prolongación analítica descendente de la superficie modelada a lo largo de 30 metros de profundidad fue usada para la optimización del modelado. Los procesos analíticos hallados fueron consistentemente útiles. La optimización de la reserva de fosfatos fue mejorada y mejor construida.

**Palabras clave:** Resistividad, fosfato, superficie de modelamiento, señal analítica, pendiente, Morocco.

## I. INTRODUCTION

Morocco is a major producer of phosphate, with an annual output of 19 million tons and reserves in excess of 35 billion cubic meters. This represents more than 75% of world reserves. Resistivity surveys have been successfully used in

the Oulad Abdoun phosphate basin in Khouribga Province (Figure 1), which is about 120 km south of Rabat. The present survey was carried out in the Sidi Chennane deposit which a part of Oulad Abdoun basin, extending over some 800 000 hectares.

\* Earth Sciences Department Faculty of Sciences & Techniques, Tangier, Morocco.  
E-mail: saad.bakkali@menara.ma

\*\* Engineering Process Department, Faculty of Sciences & Techniques, Tangier, Morocco.

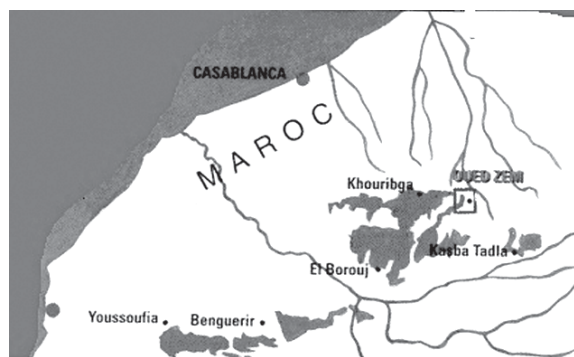


Figure 1. Location of the study area.

The Sidi Chennane deposit is sedimentary and contains several distinct phosphate-bearing layers. These layers are found in contact with alternating layers of calcareous and argillaceous hardpan. In this field, extraction was begun after Grand Daoui deposit was exhausted. However, the new deposit contains many inclusions or lenses of extremely tough hardpan locally known as *dérangements* or disturbances, found throughout the phosphate-bearing sequence. The hardpan pockets are normally detected only at the time of drilling. They interfere with field operations and introduce a severe bias in the estimates of phosphate reserves.

Direct exploration methods such as well logging or surface geology are not particularly effective. However, the chemical changes which are detectable at the hardpan/phosphate rock interface produce an important resistivity contrast. Other factors such as changes in lithofacies and clay content and consistence appear to account for some additional resistivity difference. It was found that normal phosphate-bearing rock has a resistivity of 80 to 150 W-?m while the hardpan typically features resistivity values of between 200 and 1000 W-?m. A pilot resistivity survey was performed over an area of 50 hectares. The objective of this experiment was to try and map and constrain the anomalous regions corresponding to hardpan. A resistivity map was expected to allow the electrical resistivity signals to be imaged in 3D.

## OVERVIEW OF THE AREA OF STUDY

The Sidi Chennane phosphate deposit is within the Oulad Abdoun basin about 33 km south-east of Khouribga and 24 km SSW of Oued Zem (Figure 2). Its boundaries are: West, meridian 372500 (Lambert), South, meridian 22800 (Lambert), East, highway RP22, and North, the outcrops of the

basement of the phosphate-rock sequence. The climate of the phosphate plateau is essentially arid. Rainfall is from November to May and is usually below 400 mm. Vegetation is of sparse dwarf palm trees. Rural population subsists on cattle ranching and seasonal agriculture in small villages, or douars. Ground water is increasingly scarce. Scattered wells depend on an aquifer in the Turonian limestones at depths of 100 m or more, which is sealed by the Senonian marls. This aquifer is also the sole water supply for the various mining operations.

## OVERVIEW OF THE GEOLOGICAL CONTEXT

The phosphate mineral was deposited over a long time window from Maestrichtian (late Cretaceous, about 80 ma), to Lutetian (early Eocene, 40 ma). However, deposition was irregular. Some layers are missing. Oulad Abdoun Basin occupies most of the phosphate plateau which is bounded toward the north by red outcrops of pre-Cenomanian sediments forming an extension of the south edge of the Central Massif. The Western boundary is the Rhamna Range, the Beni Amir plain is to the South and the Upper Atlas of Beni Mellal extends to the East. The geology of the study area is well understood.

The *disturbances* may be differentiated by size of the pocket or inclusion, type of material, hardness, clay content, or type of contact with the phosphate rock. Two main types of *disturbances* are found. The first type is found throughout the mineral deposit : it appears to be a random mixture of limestones, marls, clays, cherts and low-grade phosphate with large amounts of cherty limestone. The second type is highly disturbed and lacks any dominant facies. It appears as an accumulation of low-grade phosphate limestone blocks with large nodules of chert, marl, some fragments of chert and phosphate rock. The latter type forms inclusions of 10 to more than 150 m and is the most abundant during mining operations (Figure 3). These pockets



Figure 2. Main phosphate basins in Morocco.

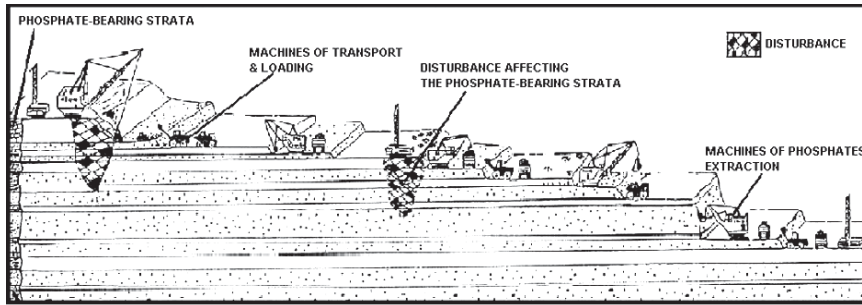


Figure 3. Adverse effects of «disturbances» on mining operations.

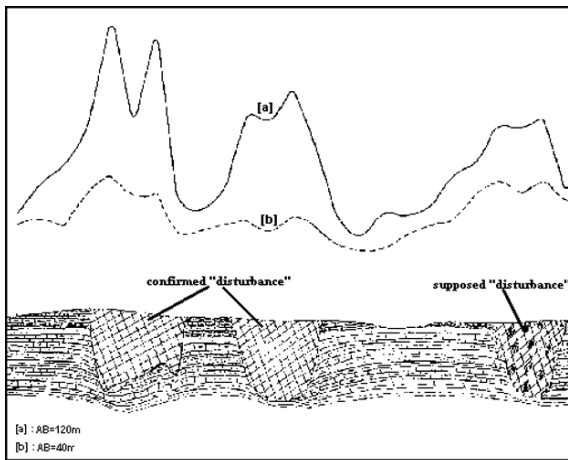


Figure 4. A resistivity traverse over three «disturbances».

are found both in the underlying formation and in the upper members of the phosphate sequence, and as a result there are strong resistivity contrasts between the *disturbances* and the normal phosphate-bearing rock. These contrasts were confirmed in the test runs (Figure 4). Geophysical prospection could thus be based on prior evidence from field data.

### FIELD PROCEDURES

Resistivity is an excellent parameter and marker for distinguishing between different types and degree of alteration of rocks. Resistivity surveys have long been successfully used by geophysicists and engineering geologists and the procedures are well established. The study area was selected for its representativity and the resistivity profiles were designed to contain both disturbed and enriched areas (Kchikach *et al.*, 1991). The sections were also calibrated by using vertical electrical soundings.

High values of apparent resistivity were encountered due to the presence of near-vertical faulting between areas of contrasting resistivity, and

fault zones which may contain more or less highly conducting fault gouge. The gouge may contain gravel pockets or alluvial material in a clay matrix (Kchikach *et al.*, 2002). Such anomalous sections are also classified as *disturbances*. Apparent resistivity values in these profiles locally exceeded 200  $\Omega\text{m}$ .

In order to locate and define the anomalous areas or *disturbances corresponding to resistivity anomalies*, an electric current of intensity  $I$  was passed between electrodes  $A$  and  $B$ , and the voltage drop  $\Delta V$  was measured between the potential electrodes  $M$  and  $N$ . The apparent resistivity is found from  $\rho_{app} = K (\Delta V / I)$ , where  $K$  is the geometric constant of the instrument which depends only on the distance between electrodes (Bakkali *et al.*, 2005). Thus the ratio between  $I$  and  $DV$  yields the resistivity of the terrain. Our Schlumberger set required the electrodes to be aligned and equidistant from the central point  $O$  so that  $MN \ll AB$ . The longer the section, the deeper is the sensitivity of the survey (Bakkali *et al.*, 2006).

The lateral inhomogeneities of the ground can be investigated by means of the apparent resistivity obtained from the survey. As the surface extension

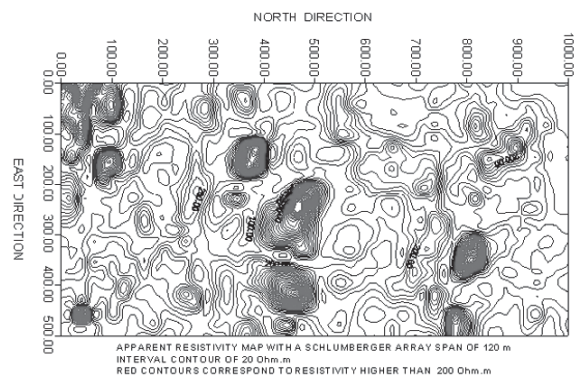


Figure 5. A map of resistivity anomalies for AB=120 m (distances in meters).

of the layers is displayed we may infer the presence or absence of any disturbances as well as any facies variations. Our resistivity measurements were performed by means of a Syscal2 resistivity meter by BRGM Instruments using a rectangular array of 20 m x 5 m. In order to reach a mean depth of exploration of 40 m we carried out 51 traverses at a spacing of 20 m (figure 5). There were 101 stations at 5 m distance for every traverse, which makes 5151 stations all together in the survey (Bakkali, 2006).

**ANALYTIC SIGNAL METHOD**

Apparent resistivity measurements are obtained from a harmonic potential  $V$  which fulfils Laplace's equation  $\nabla V=0$  in the surrounding space external to the body. The potential gradient falls off as  $1/r^2$  (Blakely, 1995). As a first approximation, the scalar potential in the neighborhood of the perturbations and within the sources complies with the equation  $\nabla V=-2rI \delta(r)$ , where  $\delta(\cdot)$  is the Dirac delta,  $r$  is the resistivity in the anomalous region and  $I$  is the current at a point electrode in an elastic halfspace, i.e. the topographic surface of the study area (Telford *et al.*, 1995). The apparent resistivity map which one obtains from such a survey is actually a map of discrete potentials on the free surface, and any major singularity in the apparent resistivities due to the presence of a perturbation will be due to the crossing from a «normal» into a «perturbed» area or vice versa. In other words, the apparent resistivity map may be considered a map of scalar potential differences assumed to be harmonic everywhere except over the perturbed areas.

Interpretation of resistivity anomalies is the process of extracting information on the position and composition of a target mineral body in the ground. In the present case the targets were

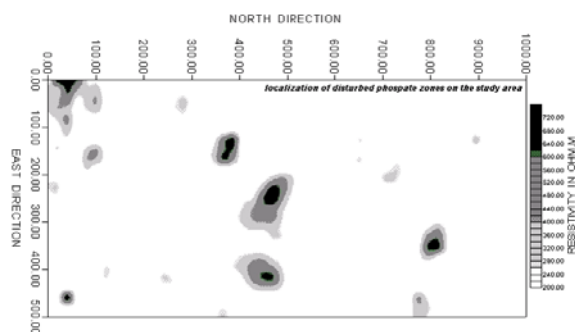


**Figure 6.** A map of disturbed phosphate zones corresponding to figure 5.

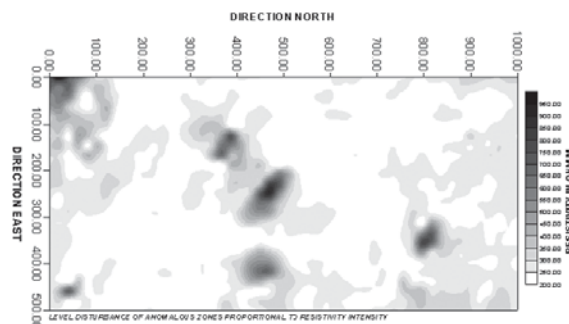


**Figure 7.** Analytique signal response of figure 6. Note the good correlation between «disturbances» and steep anomalies.

essentially the inclusions called *perturbations*. The amplitude of an anomaly may be assumed to be proportional to the volume of a target body and to the resistivity contrast with the mother lode. If the body has the same resistivity as the mother lode no anomaly will be detected. Thus assumed in fact and in first approach that the resistivity anomalies would be representative of the local density contrast between the disturbances and the mother lode. Level disturbance of the anomalous zones is proportionnal to resistivity intensity (Bakkali, 2005).

The horizontal and the vertical derivatives of the resistivity anomalies produced by a potential source form a Hilbert transform pair and define an analytic signal (Nabighian, 1972). The analytical processing method also called the total gradient method is used for defining the edges of density anomalies in terms of spatial derivatives in orthogonal directions. An important property of the 3D analytic signal is that its amplitudes is the envelope of its underlying signal (Kanasewich, 1981). It follows that the magnitude of the gradient of resistivity data is seemed to be equal to the envelope of both the horizontal and and vertical derivatives over all possible directions.

For processing resistivity data, the amplitude of the analytic signal in 3D is remarkable in that it allows one to obtain a representative signal of the resistivity anomalies over all possible directions on the study area (figure 7).

Mapped maxima in the calculated analytic signal map locate the anomalous source body edges wich correspond basically to the anomalous zones of phosphate deposit «disturbances». Analytic signal maxima have the useful property that they occur directly over singular contacts regardless of structural dip which may be present.

**EXPRESSION OF 3D ENVELOPE**

The amplitude of the analytic signal in 3D, or the total gradient, is indeed the envelope over all possible directions. Let  $A(\rho)$  be the analytic signal of the apparent resistivity both in the East and North directions. We suppose a function of  $\rho$  and  $\theta$  defined as:

$$A(\rho(x, y)) = a(x, y)\cos \theta + b(x, y)\sin \theta \quad (1)$$

where  $a(x, y)$  and  $b(x, y)$  are the directional derivatives respectively in the easting and the northing :  $a(x, y) = \frac{\partial \rho(x, y)}{\partial x}$  and

$b(x, y) = \frac{\partial \rho(x, y)}{\partial y}$ . So equation (1) can be expressed by the following terms:

$$A(\rho) = \sqrt{a^2 + b^2} \quad (2)$$

$x$  and  $y$  are the cartesian parameters of the study area, and  $\theta$  one of all possible directions. The envelope of the analytic signal of the apparent resistivity function over all values of  $\theta$  can be obtained by taking the derivative of  $A(\rho)$  with respect to  $\theta$ , setting it to zero, solving for  $\theta$  as a function of  $a$  and  $b$ , and substituting this expression into the the definition of the apparent resistivity function (Zauderer, 1989):

$$\cos \theta = \frac{\pm \frac{\partial \rho(x, y)}{\partial x}}{\sqrt{\left(\frac{\partial \rho(x, y)}{\partial x}\right)^2 + \left(\frac{\partial \rho(x, y)}{\partial y}\right)^2}} \quad (3)$$

$$\cos \theta = \frac{\pm \frac{\partial \rho(x, y)}{\partial x}}{\sqrt{\left(\frac{\partial \rho(x, y)}{\partial x}\right)^2 + \left(\frac{\partial \rho(x, y)}{\partial y}\right)^2}} \quad (4)$$

Substituting the expressions for  $\cos \theta$  and  $\sin \theta$  into equation (1) we obtained the surface envelope peaks denoted

$$\varepsilon|A(\rho(x, y))| = \sqrt{\left(\frac{\partial \rho(x, y)}{\partial x}\right)^2 + \left(\frac{\partial \rho(x, y)}{\partial y}\right)^2} \quad (5)$$

An alternate and equivalent of equation (5) is given by the following expression:

$$\varepsilon|A(\rho)| = \sqrt{|\rho|^2 + \left(\frac{\partial \rho}{\partial \theta}\right)^2} \quad (6)$$

Partial derivatives are computed numerically. The horizontal gradients are usually estimated by finite difference methods from values measured at gridded points on the apparent resistivity anomaly map using the following equations (Bakkali, 2005, 2006):

$$\frac{\partial \rho(x, y)}{\partial x} = \frac{\rho_{i+1,j} - \rho_{i-1,j}}{2\delta x} \quad \text{and} \quad \frac{\partial \rho(x, y)}{\partial y} = \frac{\rho_{i,j+1} - \rho_{i,j-1}}{2\delta y}$$

where  $x$  is the eastern coordinate and  $y$  the northern coordinate.  $\rho_{i,j}$  is the pseudo-apparent resistivity defined at grid point  $(i,j)$ . Grid intervals in the  $x$ -direction and  $y$ -direction are  $\delta x$  and  $\delta y$  respectively. In others terms surface envelope peaks are given by the following equation:

$$\left(\varepsilon|A(\rho)\right)_{i,j} = \sqrt{\left(\frac{\rho_{i+1,j} - \rho_{i-1,j}}{2\delta x}\right)^2 + \left(\frac{\rho_{i,j+1} - \rho_{i,j-1}}{2\delta y}\right)^2} \quad (7)$$

We interpolate numerically the differents obtained peaks by a surface-fit graph which represent the surface envelope of the resistivity data corresponding to the anomalous zones of the phosphate deposit disturbances. The surface-fit graph is the central point in the TableCurve 3D software used (Systat, 2002). This graph will display the  $x$ ,  $y$  and  $z$  data along with the surface for a fitted and given equation. Since optimizations are such an important part of surface science, the surface min and surface max check

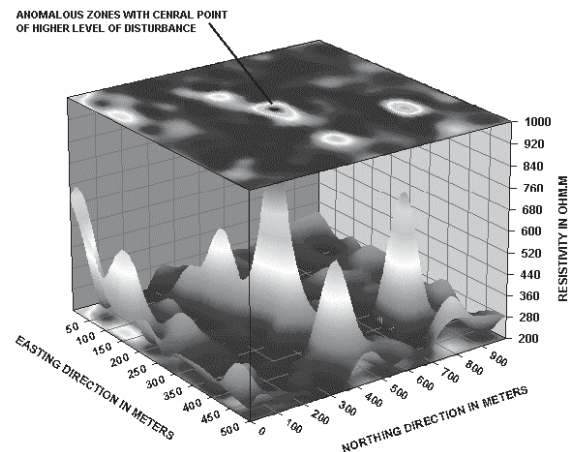


Figure 8. 3D resistivity peaks surface modeling corresponding to phosphate deposit disturbances areas.

boxes allow for the display the , and coordinates of the minimum and maximum of the surface. These are found by a two dimensional optimization algorithm (figure 8).

Figure 8 represents in this case an indicator of the level of variation of the contrast of density between the disturbances and the normal phosphate-bearing rock. The surface modeling of resistivity anomalies is obtained by the TableCurve 3D routine from our apparent resistivity survey. This procedure enables us to define the sources, after a sequence of filtering operations by analytic signal. These procedures are basically spatial filters which enhance some features of the anomaly map at the

expense of other features, thus enabling us to connect the surface anomalies to the sources at depth proportionally to resistivity peaks on the study's area.

The contrasting of density between the disturbances and the normal phosphate-bearing rock attest that the disturbances are contrasted on the surface. The overall effect is that of scanning the anomalous bodies.

Downward analytic prolongation will also amplify the effect of the deep structures, and enables us to separate the effect of adjacent sources (Bakkali, 2006). To some extent it enables

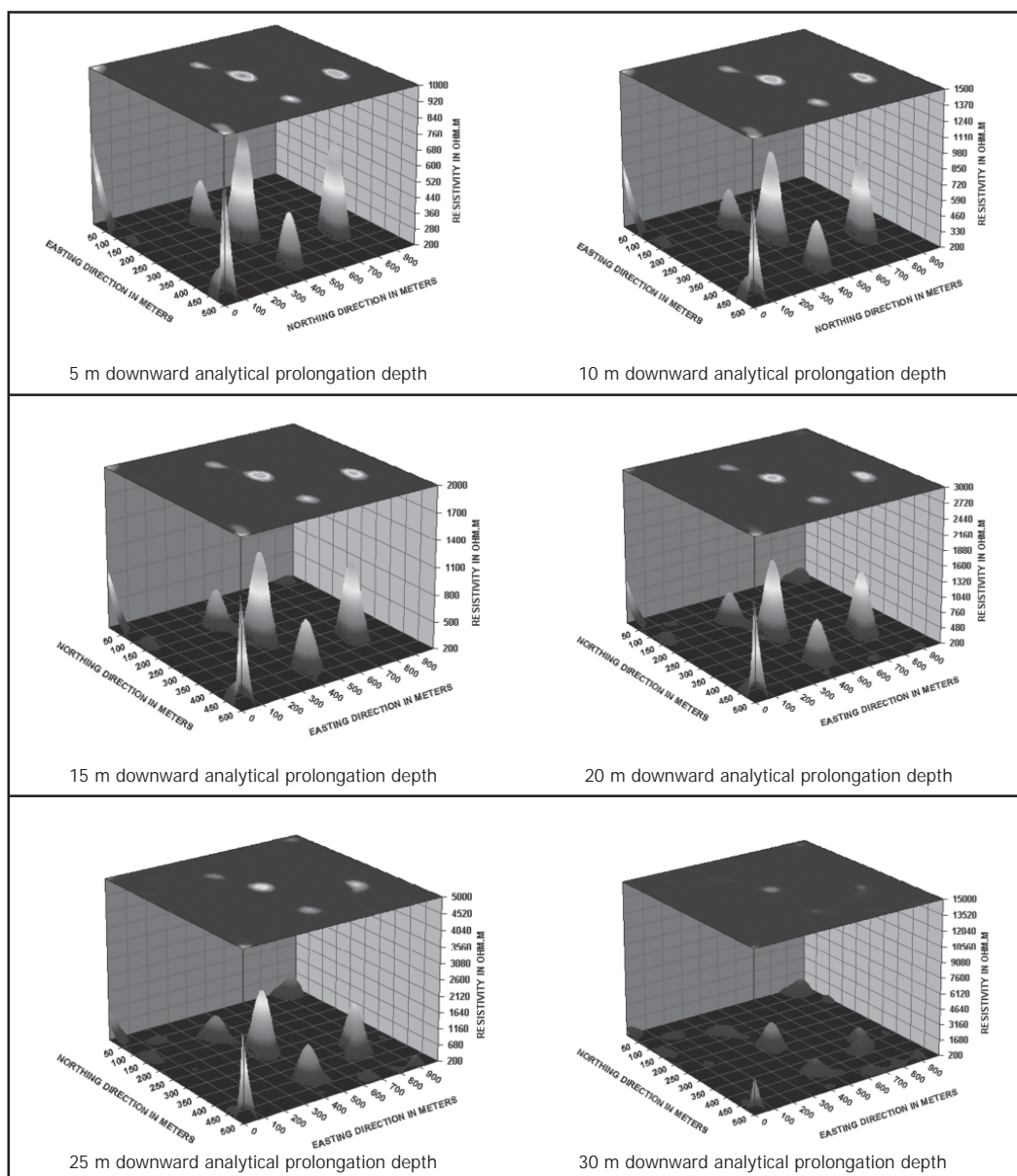


Figure 9. Downward analytic prolongation resistivity peaks surface modeling corresponding to figure 8.

us to obtain an outline of the anomalous structures and, in any case, to find the depth to the roof of the body. Of course there is a possibility to confuse several structures with a single structure (Lutz, 1999).

The data are imaged symmetrically in the space domain in order to minimize edge effects on the transformed map. Otherwise some spurious high frequency effects may appear around the edges. The downward prolongation operator may be expressed in the frequency domain by a factor  $e^{2pnz}$ , where  $z$  is the targeted depth. The frequency  $n$  may be defined as  $n = \sqrt{u^2 + v^2}$ , where  $u$  and  $v$  are the frequencies in the East and North directions (Gunn, 1975).

Once the resistivity map was filtered in the frequency domain the downward-prolonged map at a depth of 30 m was restored back to the space domain by inverse Fourier transformation. Downward prolongation was carried out in steps of 5 meters which enabled us to sample the entire sequence of the phosphate formation.

## II. RESULTS

The normalized surface resistivity maps as obtained by the above procedure in the study area provided a direct image for an interpretation of the resistivity survey (figure 9). We were able to identify the anomalies which turned out to be strongly correlated with the disturbances. We found that the disturbances as detected from surface measurements were distributed apparently at random.

The map of resistivity anomalies was enhanced with the analytical signal procedure. The anomalous areas were neatly outlined. The disturbances were outlined in depth down to 30 m. The high resistivities over anomalous areas are interpreted as reflecting the fact that the pockets of disturbed material tend to become more consolidated at depth with a less extension as modeled by the surface interpolation. We find that the downward analytic prolongation approach procedure helps to better constrain the surface location of anomalous areas. We also found that the extension in depth of the anomalous zones of phosphate deposit disturbances is limited and seem not to have an increased consistency as outlined by the downward analytical prolongation of the surface modeling. As resistivity survey with a Schlumberger device of 120 m had target 40

meters depth, it appears according to surface modeling that the anomalous zones of phosphate deposit disturbances were clearly described in the pilot study area.

## III. CONCLUSIONS

We have described an analytical procedure to identify the anomalies of a specific problem in the phosphate mining industry. The results proved satisfying. Data processing procedures as surface «disturbances» modeling using optimization of 2D peaks analytic signal of resistivity data were found to be consistently useful and the corresponding maps may be used as auxiliary tools for decision making under field conditions. The downward analytical prolongation of the surface disturbances modeling may be used by the operating personnel as a kind of radar to plan the sequence of field operations. The maps of surface «disturbances» modeling were particular useful to the surveyors for improving and constraining their 3D estimates of phosphate reserves in the deposit.

## IV. REFERENCES

1. BAKKALI, S. and L. BAHI. (2005). Cartographie des «dérangements» de séries phosphatées par mesures de résistivités électriques, *Journal des Sciences Pour l'Ingénieur, JSPI*, Vol. 6 pp1-10.
2. BLAKELY, R.J. (1995). *Potential Theory in Gravity and Magnetic Applications*, Cambridge University Press, pp 441.
3. BAKKALI, S. (2006). Application du filtrage spatial à l'analyse des contours des zones anormales de «dérangements» des séries phosphatées de Sidi Chennane (Maroc), *Revue Afrique Science*, Vol. 2, N.º 2 (under press).
4. BAKKALI, S. (2006). A resistivity survey of phosphate deposits containing hardpan pockets in Oulad Abdoun, Morocco, *Geofisica International*, 45 (1), p73-82.
5. BAKKALI, S. and L. BAHI (2006). Cartographie des «dérangements» de séries phosphatées par mesures de résistivités électriques, *Journal des Sciences Pour l'Ingénieur, J.S.P.I.*, 6, p 1-10.
6. BAKKALI, S. and J. BOUYALAOUI (2005). Essai d'optimisation de la capacité de retenue d'eau d'un lac par caractérisation géophysique du recouvrement argileux. *African Journal of Science & Technology, AJST*, 5 (2)(under press).

7. BAKKALI, S. (2005). Analysis of phosphate deposit «disturbances» using the horizontal-gradient responses of resistivity data (Oulad Abdoun, Morocco). *Earth Sci. Res. J.* Vol. 9, N.° 2, p 123-131.
8. KANASEWICH, E.R. (1981). Time sequence analysis in Geophysics. The University of Alberta Press.
9. KCHIKACH, A. and M. HIYANE. (1991). Apport de la géophysique à la détermination des dérangements à Sidi Chennane Nord, Publications Ecole Mohammadia d'Ingénieurs, Rabat, Maroc.
10. KCHIKACH, A., JAFFAL, M., AIFA, T. and BAHY, L. (2002). Cartographie de corps stériles sous couverture quaternaire par méthode de résistivités électriques dans le gisement phosphaté de Sidi Chennane (Maroc). *Comptes Rendus. Geosciences*, 334, 379-386.
11. NABIGHIAN, M.N. (1972). The analytic signal of two dimensional bodies with polygonal cross section: its properties and use for automated anomaly interpretation. *Geophysics*, 37, 507.
12. SYSTAT. (2002). About Table Curve 3DI software version 4.0, Manuel d'utilisation, Copyright Systat Software Inc, 1993-2002.
13. TELFORD, W. M. and R.E SHERIFF (1991). *Applied Geophysics*. Cambridge University Press, pp 790.
14. ZAUDERER, E. (1989). *Partial differential equations of applied mathematics*, Wiley-Interscience.